

# Applications of time-resolved terahertz spectroscopy in ultrafast carrier dynamics

(Invited Paper)

Qingli Zhou (周庆莉)<sup>1</sup> and Xicheng Zhang (张希成)<sup>2\*</sup>

<sup>1</sup>Beijing Key Laboratory for Terahertz Spectroscopy and Imaging, Key Laboratory of Terahertz Optoelectronics, Ministry of Education, Department of Physics, Capital Normal University, Beijing 100048, China

<sup>2</sup>Department of Physics, Applied Physics, and Astronomy, Center for Terahertz Research, Rensselaer Polytechnic Institute, Troy, New York 12180, USA

\*Corresponding author: zhangxc@rpi.edu

Received June 30, 2011; accepted August 8, 2011; posted online September 30, 2011

Three time-resolved terahertz (THz) spectroscopy methods (optical-pump/THz-probe spectroscopy, THz-pump/THz-probe spectroscopy, and THz-pump/optical-probe spectroscopy) are reviewed. These are used to characterize ultrafast dynamics in photo- or THz-excited semiconductors, superconductors, nanomaterials, and other materials. In particular, the optical-pump/THz-probe spectroscopy is utilized to investigate carrier dynamics and the related intervalley scattering phenomena in semiconductors. The recent development of intense pulsed THz sources is expected to affect the research in nonlinear THz responses of various materials.

OCIS codes: 300.0300, 300.6495, 300.6500.

doi: 10.3788/COL201109.110006.

## 1. Introduction

Terahertz time-domain spectroscopy (THz-TDS)<sup>[1–3]</sup> is a powerful and coherent free-space technique in which nearly single-cycle electromagnetic pulse is generated and detected using femtosecond optical pulses. THz-TDS has been utilized as one of the important methods for material characterization in the past two decades. Because transmission or reflection of THz waves is sensitive to carrier density and mobility, an ultrafast THz-TDS system is required to provide time-resolved capability of material characterization in the THz region<sup>[4–6]</sup>. In the past decade, one of the widely used time-resolved THz spectroscopy methods is optical-pump/THz-probe (O/T) spectroscopy<sup>[3]</sup>. The principle of O/T spectroscopy is premised on the idea that an optical pulse induces a change in the sample. Consequently, the resulting change in the THz signal can be measured. The advantage of O/T spectroscopy is its ability to measure directly the photo-induced changes in the photoconductivity, which contains the information on carrier density and mobility, together with a temporal resolution on the order of sub-picosecond<sup>[5]</sup>. Moreover, O/T spectroscopy technique, as one of the non-contact probe methods, has high sensitivity which facilitates the conduct of measurements under very low photo-excited carrier densities<sup>[7]</sup>. With the recent development of intense pulsed THz sources<sup>[8–10]</sup>, THz-pump/THz-probe (T/T) and THz-pump/optical-pump (T/O) spectroscopy techniques have become extended methods which are based on O/T spectroscopy. Intense THz radiation provides a new means of controlling material properties through manipulation of charge carriers, dipoles, or vibrational degrees of freedom. The new means can be applied to optical switching technology as well as THz biased devices<sup>[11]</sup>.

This the current work reviews three time-resolved THz spectroscopy methods, with an emphasis on the O/T technique and its most recent progress.

## 2. Time-resolved THz spectroscopies

### 2.1. O/T spectroscopy

Figure 1 illustrates the experimental setup of an O/T system. Based on the extension of the THz-TDS system, only the addition of an additional pump beam with time delay line (T1) is required to excite the sample. The system can be run in both 1D and 2D pump-probe schemes. Under the 1D scheme, the optical pump delay (T1) is scanned to map out the dynamics whereas the probe delay line (T2) is fixed at the peak of the THz pulse. The 1D method measures the dynamics averaged over the frequency content of the THz pulse. However, the optical pump can induce changes in the

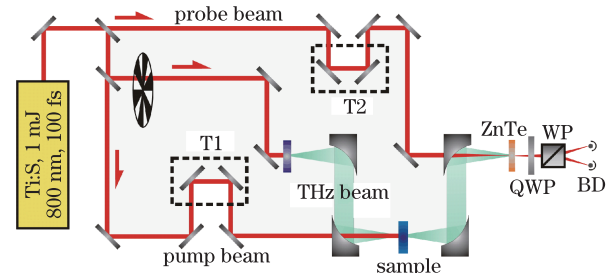


Fig. 1. Schematic experimental setup of O/T system. A regenerative amplifier system produces 800-nm pulses with 1-kHz repetition rate. The source beam is split into three portions, namely, THz generation, probe, and optical pump beams. QWP: quarter-wave plate; WP: Wollaston prism; BD: balanced detector.

amplitude and phase of the THz probe pulse. Therefore, to derive the full information of the dynamical process, 2D pump-probe scan is necessary. Generally, the 2D scan is implemented to obtain the THz waveforms by scanning the probe delay line (T2) with the optical pump delay line (T1) set at a fixed time delay  $t$  relative to the arrival of THz pulse at the sample. From the measured THz waveforms, the evolution of the photo-induced changes in the amplitude and phase of the THz electric field can be examined<sup>[3]</sup>.

The abovementioned time-resolved THz spectroscopy method has been widely used in probing the dynamics of photo-generated carriers in semiconductors<sup>[12–15]</sup>, nanomaterials<sup>[16–18]</sup>, and other materials<sup>[19,20]</sup>. Several groups have done excellent work in this field. For instance, Beard *et al.* expatiated the experimental process and measured the decay of photoconductivity in bulk GaAs with temporal resolution of 200 fs using O/T spectroscopy<sup>[7]</sup>. They obtained the electron mobilities by fitting the data to a modified Drude model. Furthermore, they found that the mobility of photo-excited electrons in low-temperature grown GaAs is lower than that in regular GaAs, and they attributed the reduction to the residual defects and strain from the excess As<sup>[21]</sup>. Subsequently, they conducted an intensive study on the ultrafast carrier dynamics in nanomaterials, such as InP nanoparticle arrays<sup>[22]</sup>, ZnO nanomaterials<sup>[23]</sup>, and TiO<sub>2</sub> nanoparticles and nanotubes<sup>[24]</sup>.

In the field of semiconductors, Liu *et al.* investigated the relaxation of photo-generated carriers in radiation-damaged silicon using a 400-nm O/T arrangement. The free-carrier density, as a function of pump time delay, and the carrier relaxation times under different pump fluences were derived<sup>[12]</sup>. Cooke *et al.* measured the laterally ordered chains of self-assembled InGaAs quantum dots and observed a large anisotropy in the transient photoconductive response<sup>[25]</sup>. In the study of dilute GaAs bismide and nitride alloys, they found that electron mobility is significantly reduced in GaNAs, with non-Drude behavior at low frequencies due to the presence of localized states<sup>[26]</sup>. The lifetime of the transient photoconductivity in the silicon nanocrystal films is dominated by trapping at interface states<sup>[27]</sup>. Moreover, they found nonlinear transient absorption bleaching of intense few-cycle THz pulses in photo-excited GaAs, due to THz electric-field-induced intervalley scattering over subpicosecond time scales. Moreover, an increase in the intravalley scattering rate due to carrier heating was observed<sup>[28]</sup>.

Schall *et al.* investigated the transmission characteristics of an air-GaAs interface and found that the total phase change and transmission of a THz probe pulse are dominated by interface effects<sup>[4]</sup>. In the study on microcrystalline silicon, Jepsen *et al.* presented direct evidence of ultrafast carrier dynamics displaying features on the picosecond time scale<sup>[29]</sup>. In 2009, Porte *et al.* observed the depletion of the conductivity via carrier capture into the quantum dots with a few picosecond pump fluence-dependent time constant when carriers are excited into the conduction band of the barriers in InGaAs/GaAs quantum dots<sup>[30]</sup>.

For the strong correlated electron materials<sup>[3,31]</sup>, Averitt *et al.* measured the transient changes in the com-

plex conductivity of YBa<sub>2</sub>Cu<sub>3</sub>O<sub>7</sub> film<sup>[32]</sup>, as well as in YBa<sub>2</sub>Cu<sub>3</sub>O<sub>7- $\delta$</sub>  thin films<sup>[33]</sup>. They presented the direct observation of photo-induced Cooper-pair breaking and the subsequent recovery dynamics of the superconducting state in MgB<sub>2</sub>. The superconducting state recovery proceeded on the timescale of several hundred picoseconds and showed strong temperature dependence, suggesting that the recovery is governed by the anharmonic decay of high-frequency acoustic phonons<sup>[34,35]</sup>. Furthermore, Kitagawa *et al.* investigated the Mott insulator YTiO<sub>3</sub> at low excitation densities and suggested that localized carriers play an important role in the incipient formation of metallic phases in photo-excited samples<sup>[36]</sup>.

Using O/T method, the transient carrier dynamics in semiconductors is investigated in this work. For CdSe, the relative change in transmission of THz peak value  $\Delta T(t)/T_0$  is monitored as a function of pump time delay under the 400-nm photo-excitation, as shown in Fig. 2, where  $\Delta T(t) = T(t) - T_0$ ,  $T(t)$  is the time-dependent transmission of THz peak value with pump, and  $T_0$  is the THz peak transmission without pump. If the THz signal is ahead of the pump pulse in time delay line T1, i.e., the time delay  $t$  is negative, then the THz peak value is unchanged, resulting in the zero value of  $\Delta T(t)/T_0$ . When the THz pulse begins to encounter the pump pulse,  $\Delta T(t)/T_0$  changes remarkably because of the photo-generated carriers in CdSe. Subsequently,  $\Delta T(t)/T_0$  recovers gradually as a result of carrier recombination. Furthermore, given that the time-dependent dynamic carrier density  $N(t)$  is proportional to  $\Delta T(t)/T(t)$ <sup>[12]</sup>, the carrier relaxation time of  $\sim 54$  ps is derived by fitting an exponential function to the carrier decay curve (not shown), as calculated based on Fig. 2. To follow the evolution of the photo-induced changes in the amplitude and phase of the THz electric field, the THz waveforms are measured at different pump time delay  $t$  obtained by 2D scan, as shown in Fig. 3. Except for the change in amplitude, no phase change in THz electric field is observed in the photo-excited CdSe.

In the semi-insulating GaAs<sup>[14]</sup>, a DC electric field ( $E$ ) is applied to the sample and the THz transmission under the 800-nm photo-excitation is monitored, as shown in Fig. 4. Surprisingly, the external  $E$  modulates the transmission of THz signal at the positive time delay, showing a significant increase in the transmission with  $E$ . Since the carrier density is very low before the pump pulse arrives, the THz peak value does not change with

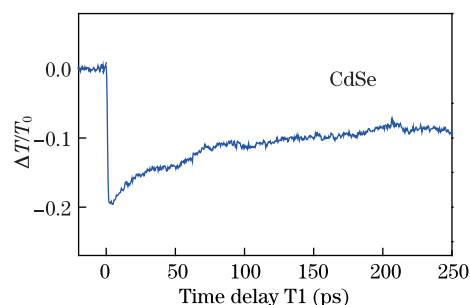


Fig. 2. Relative change in transmission of THz peak value obtained by scanning T1 with T2 set at the THz peak position (one-dimensional scan scheme). The 400-nm pump flux is  $\sim 4$  mW/cm<sup>2</sup> on 1-mm-thick undoped CdSe.

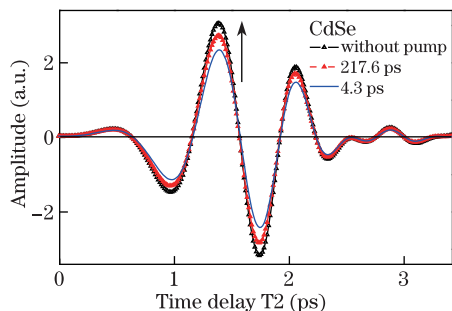


Fig. 3. THz waveforms obtained by scanning T2 with T1 set at different pump time delay position (2D scan scheme). Compared with the THz waveform through the non-excited sample, the THz signals through the photo-excited sample show an obvious decrease in amplitude at pump time delay  $t$  of 4.3 ps. Subsequently, a slight increase of 217.6 ps is observed.

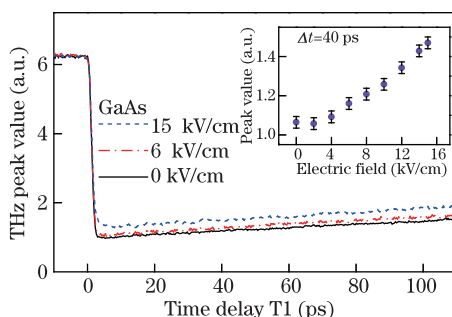


Fig. 4. 1D pump scan when T2 is fixed at the maximum value of the THz pulse under electric fields of 0, 6, and 15 kV/cm. The 800-nm pump flux is  $\sim 20$  mW/cm<sup>2</sup> on 0.5-mm-thick GaAs. The THz transmission change induced by the pump pulses at high  $E$  is smaller than the transmission without  $E$ . Inset:  $E$  dependence of the THz peak value when T1 is set at time delay of 40 ps, showing the threshold of 3–4 kV/cm when the transmission is enhanced by  $E$ .

$E$  at the negative time delay. The inset of Fig. 4 exhibits the  $E$ -dependent change in the THz peak value when the pump delay line (T1) is set at 40 ps. The threshold of  $E$  is approximately 3–4 kV/cm, corresponding to the beginning of the transmission enhancement. This phenomenon is attributed to the carrier scattering into the  $L$  valley when  $E$  exceeds the Gunn threshold (approximately 3 kV/cm in GaAs), which resulted in a reduction in carrier mobility.

## 2.2. Time-resolved THz pump spectroscopy

The availability of ultrafast high-field THz pulses provides significant opportunities for the investigation of nonlinear response of materials at THz frequencies<sup>[37–39]</sup>. For instance, Gaal *et al.* managed to observe the ultrafast nonlinear response in GaAs governed by the internal motions of quasi-particles<sup>[40]</sup>. In n-type GaAs excited by intense THz pulses, they found a long-lived coherent THz emission centered at approximately 2 THz and carrier-wave Rabi oscillations between bound impurity levels<sup>[41,42]</sup>. Furthermore, they observed THz-induced interband tunneling of electrons when they studied n-type GaAs with THz electric field strength as high as 300 kV/cm<sup>[43]</sup>.

For the T/T setup in this work, the same methodology as that in the O/T system is used. The pump beam is replaced by another intense THz beam to excite the sam-

ple. Wen *et al.*<sup>[11]</sup> used air to generate the intense THz pulses<sup>[9]</sup> and observed the nonlinear absorption and self-phase modulation of the THz pulses in InSb associated with ultrafast impact ionization processes. Hoffmann *et al.* utilized LiNbO<sub>3</sub> crystal with tilted-pulse-front method to achieve high-field THz pulses<sup>[44–46]</sup>. This method allowed them to observe a decrease in the THz absorption due to intervalley scattering in doped GaAs, Si, and Ge, as well as the impact ionization effect on InSb.

The intense THz field can strongly modify and control the optical properties of materials. T/O spectroscopy technique is a method that consists of a strong THz pulse and a weak optical probe which facilitate the study of time-resolved nonlinear effects in the optical spectral range. Danielson *et al.* performed such experiments with the wavelength of the optical probe beam centered at 805 nm to study time-resolved nonlinear effects in multiple GaAs/AlGaAs quantum wells. Pronounced spectral modulations of the light- and heavy-hole excitonic resonances were observed<sup>[47]</sup>. They demonstrated that strong THz pulses can be utilized to induce remarkable change in the optical response due to the Rabi sidebands in the semiconductor materials of the quantum wells<sup>[48,49]</sup>. Hirori *et al.* used a white-light continuum as a probe pulse to study the interaction of excitons with THz electric fields in ZnSe/ZnMgSSe multiple quantum wells. They found that the incident THz pulse induces strong spectral modulations in the heavy-hole and light-hole excitonic absorption resonances<sup>[50]</sup>.

Although THz technology has been widely used as a non-contact material characterization approach, explorations on the interaction between the intense pulses and matter have just started.

## 3. Conclusion

We review three time-resolved THz spectroscopy methods (O/T, T/T, and T/O) which are successfully applied to the studies on ultrafast carrier dynamics in the materials with emphasis on the application of O/T spectroscopy to the carrier dynamics of the semiconductor. With the recent progress in generating intense THz sources, single-cycle THz pulse with high-field strength becomes an important tool in studying directly the interaction of strong electric fields with matter at ultrafast timescales. The research of nonlinear THz spectroscopy is still at an early stage, but the prospects are becoming increasingly clear and relevant.

The authors would like to acknowledge the partial support from the Department of Energy, the National Science Foundation, and the National Natural Science Foundation of China (No. 10804077).

## References

1. D. Grischkowsky, S. R. Keiding, M. van Exter, and C. Fattinger, *J. Opt. Soc. Am. B* **7**, 2006 (1990).
2. Q. Wu and X. Zhang, *Appl. Phys. Lett.* **67**, 3523 (1995).
3. R. D. Averitt and A. J. Taylor, *J. Phys.: Condens. Matter* **14**, R1357 (2002).
4. M. Schall and P. U. Jepsen, *Opt. Lett.* **25**, 13 (2000).
5. S. E. Ralph, Y. Chen, J. Woodall, and D. McInturff,

- Phys. Rev. B **54**, 5568 (1996).
6. S. S. Prabhu, S. E. Ralph, M. R. Melloch, and E. S. Harmon, Appl. Phys. Lett. **70**, 2419 (1997).
  7. M. C. Beard, G. M. Turner, and C. A. Schmuttenmaer, Phys. Rev. B **62**, 15764 (2000).
  8. K. Y. Kim, J. H. Glowia, A. J. Taylor, and G. Rodriguez, Opt. Express **15**, 4577 (2007).
  9. X. Xie, J. Dai, and X. Zhang, Phys. Rev. Lett. **96**, 075005 (2006).
  10. J. Dai, X. Xie, and X. Zhang, Phys. Rev. Lett. **97**, 103903 (2006).
  11. H. Wen, M. Wiczer, and A. M. Lindenberg, Phys. Rev. B **78**, 125203 (2008).
  12. K. P. H. Liu and F. A. Hegmann, Appl. Phys. Lett. **78**, 3478 (2001).
  13. J. Lloyd-Hughes, S. K. E. Merchant, L. Fu, H. H. Tan, C. Jagadish, E. Castro-Camus, and M. B. Johnston, Appl. Phys. Lett. **89**, 232102 (2006).
  14. Q. Zhou, Y. Shi, B. Jin, and C. Zhang, Appl. Phys. Lett. **93**, 102103 (2008).
  15. L. Fekete, P. Kužel, H. Němec, F. Kadlec, A. Dejneka, J. Stuchlík, and A. Fejfar, Phys. Rev. B **79**, 115306 (2009).
  16. P. Parkinson, J. Lloyd-Hughes, Q. Gao, H. H. Tan, C. Jagadish, M. B. Johnston, and L. M. Herz, Nano Lett. **7**, 2162 (2007).
  17. P. A. George, J. Strait, J. Dawlaty, S. Shivaraman, M. Chandrashekar, F. Rana, and M. G. Spencer, Nano Lett. **8**, 4248 (2008).
  18. J. H. Strait, P. A. George, M. Levendorf, M. Blood-Forsythe, F. Rana, and J. Park, Nano Lett. **9**, 2967 (2009).
  19. H. Němec, H.-K. Nienhuys, F. Zhang, O. Inganäs, A. Yartsev, and V. Sundström, J. Phys. Chem. C **112**, 6558 (2008).
  20. P. D. Cunningham, L. M. Hayden, H.-L. Yip, and A. K.-Y. Jen, J. Phys. Chem. B **113**, 15427 (2009).
  21. M. C. Beard, G. M. Turner, and C. A. Schmuttenmaer, J. Appl. Phys. **90**, 5915 (2001).
  22. M. C. Beard, G. M. Turner, J. E. Murphy, O. I. Micic, M. C. Hanna, A. J. Nozik, and C. A. Schmuttenmaer, Nano Lett. **3**, 1695 (2003).
  23. J. B. Baxter and C. A. Schmuttenmaer, J. Phys. Chem. B **110**, 25229 (2006).
  24. C. Richter and C. A. Schmuttenmaer, Nat. Nanotechnol. **5**, 769 (2010).
  25. D. G. Cooke, F. A. Hegmann, Y. I. Mazur, W. Ma, X. Wang, Z. Wang, G. J. Salamo, M. Xiao, T. D. Mishima, and M. B. Johnson, Appl. Phys. Lett. **85**, 3839 (2004).
  26. D. G. Cooke, F. A. Hegmann, E. C. Young, and T. Tiedje, Appl. Phys. Lett. **89**, 122103 (2006).
  27. D. G. Cooke, A. N. MacDonald, A. Hryciw, A. Meldrum, J. Wang, Q. Li, and F. A. Hegmann, J. Mater. Sci.: Mater. Electron **18**, S447 (2007).
  28. F. H. Su, F. Blanchard, G. Sharma, L. Razzari, A. Ayesheshim, T. L. Cocker, L. V. Titova, T. Ozaki, J. C. Kieffer, R. Morandotti, M. Reid, and F. A. Hegmann, Opt. Express **17**, 9620 (2009).
  29. P. U. Jepsen, W. Schairer, I. H. Libon, U. Lemmer, N. E. Hecker, M. Birkholz, K. Lips, and M. Schall, Appl. Phys. Lett. **79**, 1291 (2001).
  30. H. P. Porte, P. UhdJepsen, N. Daghestani, E. U. Rafailov, and D. Turchinovich, Appl. Phys. Lett. **94**, 262104 (2009).
  31. R. D. Averitt, A. I. Lobad, C. Kwon, S. A. Trugman, V. K. Thorsmølle, and A. J. Taylor, Phys. Rev. Lett. **87**, 017401 (2001).
  32. R. D. Averitt, G. Rodriguez, J. L. W. Siders, S. A. Trugman, and A. J. Taylor, J. Opt. Soc. Am. B **17**, 327 (2000).
  33. R. D. Averitt, G. Rodriguez, A. I. Lobad, J. L. W. Siders, S. A. Trugman, and A. J. Taylor, Phys. Rev. B **63**, 140502(R) (2001).
  34. J. Demsar, R. D. Averitt, A. J. Taylor, W.-N Kang, H. J. Kim, E.-M. Choi, and S.-I. Lee, Int. J. Mod. Phys. B **17**, 3675 (2003).
  35. J. Demsar, R. D. Averitt, and A. J. Taylor, J. Supercond. Nov. Magn. **17**, 143 (2004).
  36. J. Kitagawa, Y. Kadoya, M. Tsubota, F. Iga, and T. Takabatake, J. Phys.: Condens. Matter **19**, 406224 (2007).
  37. J. Hebling, K. Yeh, M. C. Hoffmann, and K. A. Nelson, IEEE J. Sel. Top. Quantum Electron. **14**, 345 (2008).
  38. M. C. Hoffmann and J. A. Fülöp, J. Phys. D: Appl. Phys. **44**, 083001 (2011).
  39. J. A. Fülöp, L. Pálfalvi, G. Almási, and J. Hebling, J. Infrared Millim. Terahertz Waves **32**, 553 (2011).
  40. P. Gaal, W. Kuehn, K. Reimann, M. Woerner, T. Elsaesser, and R. Hey, Nature **450**, 1210 (2007).
  41. P. Gaal, K. Reimann, M. Woerner, T. Elsaesser, R. Hey, and K. H. Ploog, Phys. Rev. Lett. **96**, 187402 (2006).
  42. P. Gaal, W. Kuehn, K. Reimann, M. Woerner, T. Elsaesser, R. Hey, J. S. Lee, and U. Schade, Phys. Rev. B **77**, 235204 (2008).
  43. W. Kuehn, P. Gaal, K. Reimann, M. Woerner, T. Elsaesser, and R. Hey, Phys. Rev. B **82**, 075204 (2010).
  44. M. C. Hoffmann, J. Hebling, H. Y. Hwang, K.-L. Yeh, and K. A. Nelson, Phys. Rev. B **79**, 161201 (2009).
  45. M. C. Hoffmann, J. Hebling, H. Y. Hwang, K.-L. Yeh, and K. A. Nelson, J. Opt. Soc. Am. B **26**, A29 (2009).
  46. J. Hebling, M. C. Hoffmann, H. Y. Hwang, K.-L. Yeh, and K. A. Nelson, Phys. Rev. B **81**, 035201 (2010).
  47. J. R. Danielson, Y.-S. Lee, J. P. Prineas, J. T. Steiner, M. Kira, and S. W. Koch, Phys. Rev. Lett. **99**, 237401 (2007).
  48. A. D. Jameson, J. L. Tomaino, Y.-S. Lee, J. P. Prineas, J. T. Steiner, M. Kira, and S. W. Koch, Appl. Phys. Lett. **95**, 201107 (2009).
  49. J. L. Tomaino, A. D. Jameson, Y.-S. Lee, J. P. Prineas, J. T. Steiner, M. Kira, and S. W. Koch, Solid State Electron. **54**, 1125 (2010).
  50. H. Hirori, M. Nagai, and K. Tanaka, Phys. Rev. B **81**, 081305(R) (2010).